

New pink ceramic pigment based on chromium (IV)-doped lutetium gallium garnet

R. Galindo, M. Llusar, M.A. Tena, G. Monrós, J.A. Badenes*

Inorganic Chemistry Area, Inorganic and Organic Department, Jaume I University, 12071 Castellón, Spain

Received 22 September 2005; received in revised form 27 January 2006; accepted 17 February 2006

Available online 19 April 2006

Abstract

Lutetium gallium garnet codoped with chromium and calcium (Ca,Cr:LGG) and lutetium gallium garnet with chromium as single dopant (Cr:LGG) have been studied. Samples with $\text{Ca}_x\text{Cr}_x\text{Lu}_{3-2x}\text{Ga}_5\text{O}_{12}$ ($x = 0, 0.05, 0.10, 0.15, 0.2, 0.4, 0.6$) and $\text{Cr}_x\text{Lu}_{3-x}\text{Ga}_5\text{O}_{12}$ ($x = 0.15$ and 0.6) compositions were prepared by solid state reaction and the fired samples ($1250^\circ\text{C}/6\text{ h}$) were characterised by XRD, lattice parameters determination, UV–vis–NIR spectroscopy, CIEL*a*b* measurements and SEM/EDX. Moreover, the samples with calcium were tested as ceramic pigments in a conventional glaze matrix. In the Ca,Cr:LGG system solid solutions incorporating both Cr(III) and Cr(IV) ions were obtained. Cr(IV) occupies basically dodecahedral sites substituting for Lu (III) and is the predominant oxidation state up to $x = 0.20$ composition, giving a pink colouration in the ceramic glaze matrix. In the Cr:LGG system, only Cr(III) enters in solid solution occupying octahedral positions and producing green shades. © 2006 Elsevier Ltd. All rights reserved.

Keyword: Gallium garnet; Powders-solid state reaction; Spectroscopy; Colour; Pigments; $\text{Lu}_3\text{Ga}_5\text{O}_{12}$

1. Introduction

One of the most important host lattices for solid state lasers is found to be the garnet structure because the resulting materials are chemically stable, mechanically hard and have good thermal and optical properties. Therefore, materials based on aluminium or gallium garnets such as $\text{Y}_3\text{Al}_5\text{O}_{12}$ (YAG), $\text{Lu}_3\text{Al}_5\text{O}_{12}$ (LAG), $\text{Y}_3\text{Ga}_5\text{O}_{12}$ (YGG), $\text{Gd}_3\text{Ga}_5\text{O}_{12}$ (GGG), $\text{Gd}_3\text{Sc}_2\text{Ga}_3\text{O}_{12}$ (GSGG), $\text{La}_3\text{Lu}_2\text{Ga}_3\text{O}_{12}$ (LLGG), $\text{Y}_3\text{Sc}_2\text{Ga}_3\text{O}_{12}$ (YSGG) have been widely studied.^{1–4} Garnet crystals are cubic and belong to the space group Ia3d. The garnet crystal is schematically formulated as $[\text{A}_3][\text{B}_2][\text{C}_3]\text{O}_{12}$ where “A”, “B” and “C” denote trivalent cation sites, dodecahedrally, octahedrally and tetrahedrally coordinated, respectively. Oxide garnets can achieve systematic changes in the crystal field strength by variation of the unit-cell size. Along the series YAG, YGG, GGG, GSGG and LLGG the unit cell size increases and the crystal field strength decreases progressively.¹ Gallium garnets are especially interesting for scintillator applications since, as compared to aluminium garnets, they have a larger unit cell volume, higher

density and belong to compositionally disordered compounds due to a high solubility of the rare-earth ion in the octahedral sites.⁵ In this sense, lanthanum lutetium gallium garnets (LLGG)^{6,7} and lutetium gallium garnets (LGG)^{8,9} have been studied recently.

These garnet structures are normally doped with neodymium, ytterbium and chromium as laser active ions. As single dopants, these cations enter in aluminium and gallium garnets as trivalent ions, occupying the octahedral sites. However, in chromium-doped garnets the effective laser ion is Cr^{4+} , and the stabilisation of this oxidation state of chromium is only obtained if the garnet is codoped with a divalent cation to compensate the charge. Ca^{2+} or Mg^{2+} are often used for this purpose, but other divalent cations fail to stabilise Cr(IV) due to the large crystal field stabilisation energy for Cr^{3+} in octahedral sites. The role of Ca^{2+} is well known in YAG and GGG¹⁰ and no more than 1 mol.% of Ca ions become effective to stabilise Cr(IV).¹¹ Cr^{4+} and Ca^{2+} ions enter in “C” tetrahedral and “A” dodecahedral sites of the YAG lattice, respectively. But recent studies indicate the Cr^{4+} may reside in both octahedral and tetrahedral positions.¹² It is commonly assumed¹³ that only 2% of the chromium, with a total Cr concentration of 0.2 mol.%, is tetrahedrally coordinated Cr^{4+} . Consequently, both Cr^{4+} and Cr^{3+} are contained in Ca,Cr:YAG system and the existence of

* Corresponding author. Fax: +34 964728214.

E-mail address: jbadenes@qio.uji.es (J.A. Badenes).

Cr^{6+} or Cr^{5+} in samples is not discarded depending on synthesis conditions.

On the other hand, chromium is the most versatile chromophore used in ceramic pigments: chrome alumina pink corundum (DCMA 3-03-5), chromium green-black hematite (DCMA 3-05-3), chrome tin pink sphene (DCMA 12-25-5), zinc chrome cobalt aluminium blue spinel (DCMA 13-53-2), chrome iron black spinel (DCMA 13-50-9), victoria green the unique garnet catalogued in DCMA (4-07-3) . . . Its variety of oxidation states depending on the host lattice and synthesis conditions explain this versatility. In addition, since Cr^{3+} is highly stabilised in octahedral sites, the colour can be shifted to red shades by modulating this octahedral environment towards a stronger crystal field, as it occurs in $\text{Cr}_2\text{O}_3\text{-Al}_2\text{O}_3$ or YAlO_3 pigments.¹⁴

Nowadays, the garnet structure is investigated as host lattice to develop new ceramic pigments. Its suitable properties such as chemical stability, mechanical hardness, good thermal and optical behaviour, and the possibility to change the crystal field strength for the chromophore ion lead to it. Indeed, red pigments based on Ca,Cr:YAG^{15} and Ca,Cr:GGG^{16} have been reported recently.

The aim of this work is to study the potential use of Ca,Cr:LGG system as ceramic pigment, also analysing the crystal coordination and valence of chromium ions in the solid solution.

2. Experimental procedure

Samples with a molar composition $\text{Ca}_x\text{Cr}_x\text{Lu}_{3-2x}\text{Ga}_5\text{O}_{12}$ ($x=0, 0.05, 0.10, 0.15, 0.2, 0.4, 0.6$) in the Ca,Cr:LGG system and $\text{Cr}_x\text{Lu}_{3-x}\text{Ga}_5\text{O}_{12}$ ($x=0.15$ and 0.6) composition in the Cr:LGG system were prepared. All samples were synthesised by solid state reaction using CaCO_3 , Cr_2O_3 , Lu_2O_3 and Ga_2O_3 as Ca , Cr , Lu and Ga precursors. All of them were analytical reagents supplied by Aldrich. The raw materials were ball-milled in acetone for 20 min. Residual acetone was then removed by evaporation, and the resulting dried powder was finally homogenized in an agate mortar. Samples were fired at 1250°C with 6 h of soaking time. The reference of each composition is given in Table 1.

Samples were also washed and the Cr(VI) content was measured in the washing liquids of the samples. With this purpose,

Table 1
References of studied samples

Composition $\text{Ca}_x\text{Cr}_x\text{Lu}_{3-2x}\text{Ga}_5\text{O}_{12}$	Reference
$X=0$	LG00
$X=0.05$	LG05
$X=0.1$	LG10
$X=0.15$	LG15
$X=0.2$	LG20
$X=0.4$	LG40
$X=0.6$	LG60
$\text{Cr}_x\text{Lu}_{3-x}\text{Ga}_5\text{O}_{12}$	
$X=0.15$	LG15V
$X=0.6$	LG60V

1 g of fired sample was ground and washed using boiling water and continuous stirring during one hour. The Cr(VI) content in 200 mL of washing water was determined by a colourimetric method using diphenylcarbazide. Measurements were conducted on the spectrophotometer used for $\text{CIE } L^*a^*b^*$ measurements at 540 nm.

X-ray diffraction (XRD) patterns were obtained in a Siemens D-500 diffractometer with Ni filtered $\text{Cu K}\alpha$ radiation. Lutetium gallium garnet cell parameters were measured using $\alpha\text{-Al}_2\text{O}_3$ as internal standard by the POWCAL and LSQC calculation programmes.¹⁷

UV–vis–NIR spectroscopy (diffuse reflectance) of fired samples and enameled samples also was performed with a Perkin-Elmer (Lambda 2000) spectrophotometer at a range between 200 and 1600 nm. In addition, $L^*a^*b^*$ colour parameters of both fired powders and enameled samples were measured with the same Perkin-Elmer spectrophotometer using a standard lighting C, following the $\text{CIE-L}^*a^*b^*$ colourimetric method recommended by CIE (Comission International de l'Eclairage).¹⁸ On this method, L^* is the lightness axis, a^* is the green (–)→ red (+) axis, and b^* is the blue (–)→ yellow (+) axis.

The microstructure and chemical homogeneity of representative fired samples were studied by Scanning Electron Microscopy (SEM), using a Leo-440i Leyca electron microscope equipped with an Energy Dispersion X-ray (EDX) attachment by Oxford University. The EDX analyses allowed us to study the elements distribution in the samples.

To test their efficiency as ceramic pigments, fired samples were 5% enameled with a transparent single-firing glaze into ceramic biscuits, and then fired following a fast fired scheme (52 min of duration cool to cool at a maximum temperature of 1085°C).

3. Results and discussion

3.1. XRD results

The phases detected by XRD in fired samples at $1250^\circ\text{C}/6\text{ h}$ are given in Table 2. All samples present lutetium gallium garnet as the main crystalline phase. Only in LG00 sample, unreacted Lu_2O_3 and Ga_2O_3 are detected and the garnet peaks intensity is the lowest. As may be seen in Fig. 1, the presence of chromium increases the reactivity of the system to yield the garnet crystalline phase with respect to the sample without chromium. Table 2 shows that crystal garnet is the only phase detected from LG05 to LG15 samples, while Ga_2O_3 as secondary phase and unknown peaks are detected from LG20 to LG60. These peaks are associated to some crystalline phase containing calcium because they are not detected in samples without this metal. The presence of other crystalline phases together with garnet indicates the unstabilisation of the formulated Ca,Cr:LGG solid solution from LG20 sample.

3.2. Analysis of Cr(VI) in washing liquids

The washing process allows us to eliminate the toxic ion Cr(VI) from the fired powders. The measures of leached Cr(VI)

Table 2

Crystalline phases detected by XRD, Cr(VI) amount measured in leached water (per gram of sample) and LGG cell parameters (values between brackets are the estimated standard deviation) in fired samples at 1250 °C/6 h

Sample	Crystalline phases	mg Cr(VI)/g	Lattice parameters (Å) $a=b=c=12.183^*$
LG00	G(m)L(w)Ga(w)	0	12.189(3)
LG05	G(s)	0.010	12.193(3)
LG10	G(s)	0.021	12.193(2)
LG15	G(s)	0.035	12.193(2)
LG20	G(s)Ga(w)	0.065	12.194(3)
	X ₂ (vw)X ₄ (vw)		
	X ₅ (vw)X ₆ (vw)		
LG40	G(s)Ga(w)	0.095	12.191(2)
	X ₂ (vw)X ₃ (vw)X ₄ (vw)		
	X ₅ (vw)X ₆ (vw)		
LG60	G(s)Ga(w)	0.140	12.192(2)
	X ₅ (w)X ₂ (vw)		
	X ₃ (vw)X ₄ (vw)X ₆ (vw)		
LG15V	G(vs)Ga(vw)	0.023	12.1765(2)
LG60V	G(vs)Ga(m)	NM	12.1764(5)

Crystalline phases: G (Lu₃Ga₅O₁₂), Ga (Ga₂O₃), L (Lu₂O₃). X = unassigned peaks: X₂ ($2\theta = 19.7^\circ$), X₃ ($2\theta = 25.1^\circ$), X₄ ($2\theta = 28.2^\circ$), X₅ ($2\theta = 34.9^\circ$), X₆ ($2\theta = 25.8^\circ$). Intensity peak: vs (very strong), s (strong), m (medium), w (weak), vw (very weak). NM = non measured. *JCPDS card 13–00.

are given in Table 2. The results indicate that the presence of Cr(VI) in leaching waters increases with the amount of chromium in the formulation increases.

3.3. UV–vis–NIR spectroscopy

The UV–vis–NIR spectra of samples containing calcium and fired at 1250 °C/6h are given in Fig. 2. In general, the spec-

tra present similar features, and the intensity of the absorption peaks increase with chromium concentration. For the three regions of spectra, the following considerations must be pointed out: (a) an intense sharp band is observed in the ultraviolet region, (b) the visible region is dominated by a broad band centred at 420–450 nm, together with other two bands at 620 and 680 nm presenting a higher intensity when the Cr amount increases c) NIR region presents three weak bands centred around 900, 1000 and 1120 nm, and a band around 1450 nm which is specially intense in LG10 and LG15 samples.

The spectra of LG05, LG10 and LG15 samples are characterised by a band centred at 420 nm and a wide band between 900 and 1200 nm that can be associated to Cr⁴⁺ in dodecahedral positions.¹⁶ Both bands present an increasing absorbance from LG05 to LG15. When the Cr amount is increased (from LG20) and the LGG phase is accompanied by other crystalline phases

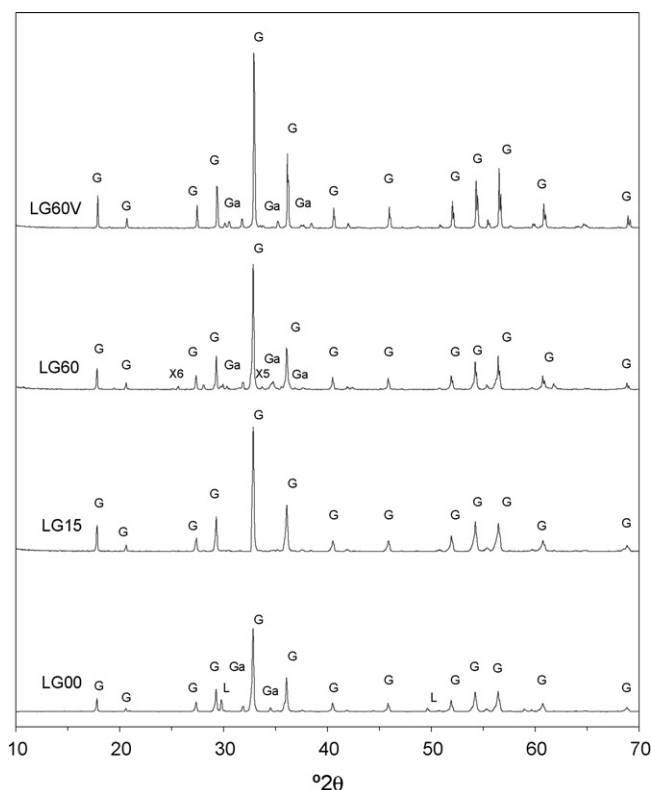


Fig. 1. XRD of representative samples fired at 1250 °C/6 h.

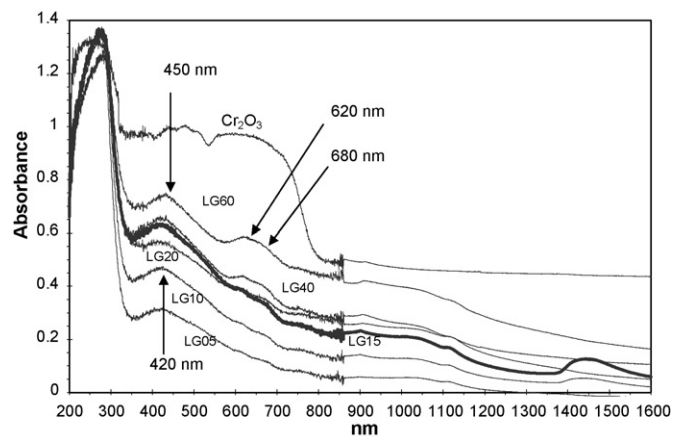


Fig. 2. UV–vis–NIR spectra of powders fired at 1250 °C/6 h. The spectrum of Cr₂O₃ is given as a reference. The strongest line spectrum is associated to LG15 sample.

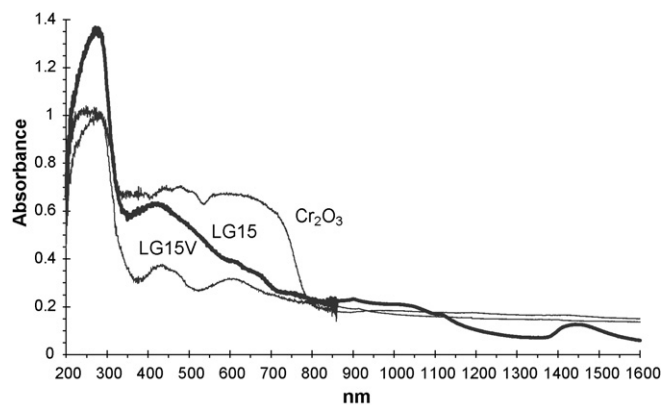


Fig. 3. UV-vis-NIR spectra of samples with calcium (LG15) and without calcium (LG15V). The spectrum of Cr_2O_3 is given as a reference.

(see Table 2), the intensity of the band at 420 nm decreases (in LG15 this band is more intense than in LG20) and shifts to higher wavelength up to 450 nm in LG60 as is indicated in Fig. 2. Also from LG20, two bands at 620 and 680 nm develop their absorbance intensity due to the overlapping of bands associated to Cr^{4+} and Cr^{3+} . In LG40 and LG60 the spectra are dominated by bands associated to Cr^{3+} in octahedral sites, and their spectra are more similar to that of sample without calcium given in Fig. 3.

Fig. 3 shows the spectra of samples LG15 and LG15V to compare the influence of calcium on the chromophore ion in the crystalline garnet. As may be appreciated the sample without calcium (LG15V) presents two broad absorption bands centred at 420 and 620 nm dominating the visible region, being the spectrum very different to its homologue with calcium (LG15).

The LG15V spectrum can be explained only by the presence of Cr^{3+} . The bands at 420 and 620 nm are attributed to the $4\text{A}_2 \rightarrow 4\text{T}_1(4\text{F})$ and $4\text{A}_2 \rightarrow 4\text{T}_2$ transitions of Cr^{3+} in octahedral sites, respectively.¹⁹ Moreover, the band at 680 nm that appears from LG15 to LG60 and is not present in samples without calcium can be assigned to the $3\text{A}_2 \rightarrow 3\text{T}_1(3\text{F})$ transition of Cr^{4+} in tetrahedral coordination.

From these results, when Cr and Ca are introduced into the LGG crystal there are two main oxidation states: Cr(IV) and Cr(III). Cr(IV) in dodecahedral sites dominates the spectrum when the chromium concentration is relatively small, however from LG20 to LG60 the spectra also indicates the presence of Cr(IV) but the visible region are more and more similar to a spectrum dominated by Cr(III) in octahedral positions.

3.4. Lattice cell parameters

The cell parameters calculated by POWCAL and LSQC programmes are given in Table 2. Attending to the ionic radius proposed by Shannon²⁰ for Cr^{3+} (0.755 Å) and Ga^{3+} (0.76 Å) in octahedral sites, the substitution of Ga^{3+} by Cr^{3+} does not modify cell parameters substantially. In samples without calcium, the results given in Table 2 show a decrease

Table 3

CIEL*a*b* colourimetric parameters of samples fired at 1250 °C/6 h and of enameled samples in a transparent glaze with 5% of pigment

Sample	Powders			Enameled samples		
	L^*	a^*	b^*	L^*	a^*	b^*
LG00	100	0	0	91.7	1.3	6.7
LG05	82.3	3.4	9.7	87.6	1.9	11.4
LG10	71.7	4.6	13.4	77.1	4.1	14.5
LG15	64.7	4.7	14.5	72.9	5.1	17.0
LG20	70.0	3.7	14.0	65.9	5.9	14.7
LG40	64.6	1.7	13.8	57.5	4.4	13.9
LG60	61.5	−1.1	12.5	51.5	2.0	10.8
LG15V	81.9	−14.5	13.5	NE	NE	NE
LG60V	85.9	−12.6	13.2	NE	NE	NE

NE: no enameled.

of cell parameters with respect to LG00 sample which are in accordance with the Cr^{3+} (0.755 Å) occupying the octahedral positions of Lu^{3+} (1.001 Å).⁹ When Lu^{3+} octahedral sites become saturated, the Cr^{3+} occupies the Ga^{3+} octahedral positions and the cell parameters do not change as it is observed when comparing LG60V with respect to LG15V sample.

The interpretation in Ca,Cr:LGG system is more difficult because the chromium is found in different positions and in two oxidation states according to UV-vis-NIR results. The entrance of Ca^{2+} substituting for Lu^{3+} sites in dodecahedral positions produces an increase of cell parameters considering the ionic radii proposed by Shannon ($r_{\text{Ca}}[\text{VIII}] = 1.26$ Å, $r_{\text{Lu}}[\text{VIII}] = 1.117$ Å). However, the entrance in the lattice of a small sized cation such as Cr^{4+} also produces a contraction of cell parameters compensating the effect of Ca^{2+} entrance; this explain that the lattice values remain unchanged up to LG15 composition. From LG20 sample when the chromium enters in solid solution basically as Cr^{3+} substituting for Ga^{3+} in octahedral sites the lattice parameters do not change because their corresponding ionic radii are similar.

These results are in agreement with optical spectra and DRX data. DRX results show that $\text{Lu}_3\text{Ga}_5\text{O}_{12}$ is the only crystalline phase detected from LG05 to LG15 compositions, and optical spectra indicate that Cr^{4+} is predominantly in dodecahedral position up to LG15, being from this composition when the bands around 620–680 nm become progressively more intense.

The Cr(IV) substituting for Lu(III) is stabilised using calcium as charge compensator in LGG garnet. In samples without calcium addition, Ga_2O_3 is detected by XRD as residual crystalline phase and Cr^{3+} in octahedral coordination is observed from optical spectra, in agreement with the entrance of Cr^{3+} in the garnet lattice substituting for Ga^{3+} .

3.5. CIEL*a*b* measurements

The colour parameters ($L^*a^*b^*$) of the fired powders are given in Table 3. The evolution of a^* and b^* parameters with the composition may also be seen in Fig. 4. The colour of pow-

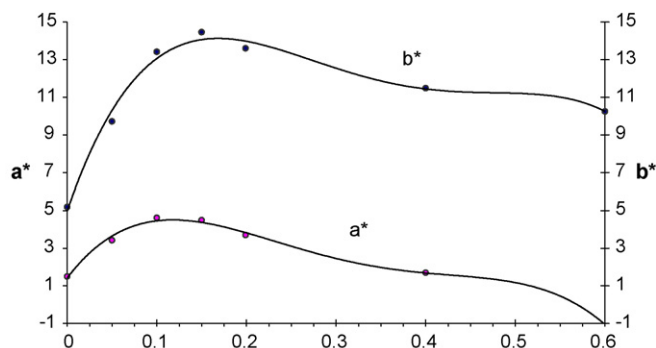


Fig. 4. Evolution of a^* and b^* colour parameters with composition in the Ca,Cr:LGG system.

der samples without calcium addition are light green ($L^* = 85.9$, $a^* = -12.6$, $b^* = 13.2$). This is in agreement with the presence of Cr^{3+} in octahedral coordination substituting for Ga^{3+} , as it is above described. However, in Ca,Cr:LGG solid solution the results given in Fig. 4 show higher values of a^* and b^* colour parameters giving rise to pinker colourations. The pink colour is observed just up to $x = 0.2$ compositions (LG20 sample: $L^* = 70.0$, $a^* = 3.7$, $b^* = 14.0$) but for samples richer in chromium the colour of powders become greenish, since the solid solutions are saturated and Cr^{3+} substitutes for Ga^{3+} in octahedral sites.

3.6. Evaluation of Ca,Cr:LGG as ceramic pigment

In order to evaluate the performance of Ca,Cr:LGG as ceramic pigment all samples were enameled following the conditions described in experimental procedure. The UV–vis–NIR spectra of enameled samples are shown in Fig. 5. The results indicate that the chromium (IV) lutetium gallium garnet resists the enameling process. The evolution of CIEL $^*a^*b^*$ parameters in glazed samples (given in Table 3) are similar to that described for powders: the pink colour enhances when chromium and calcium enter in solid solution up to LG20 sample, and a greenish colour is obtained when Cr^{3+} enters in Cr-enriched samples. Accordingly, the obtained Ca,Cr:LGG solid solutions

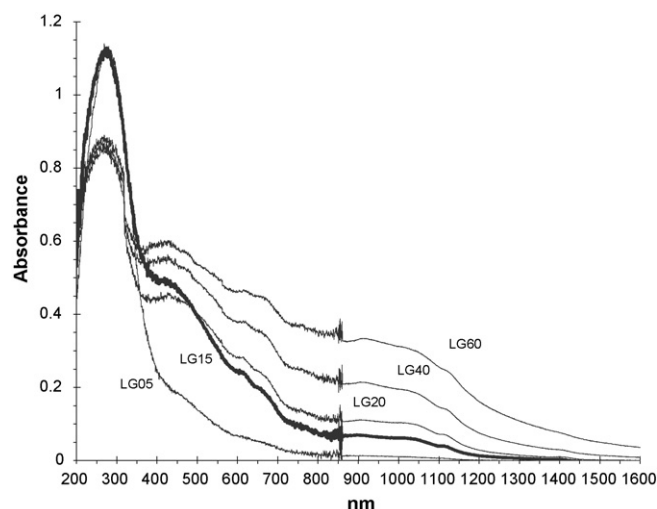


Fig. 5. UV–vis–NIR spectra of enameled samples. The strongest line spectrum is associated to LG15 sample.

are useful as pink ceramic pigment on glaze media up to $x = 0.2$ composition.

3.7. Microstructure characterization

The microstructure of representative samples fired at $1250^\circ\text{C}/6\text{ h}$ is shown in Fig. 6. LG15 sample shows a wide distribution of agglomerate sizes from 1 to $3\ \mu\text{m}$ though the particles may not be clearly distinguished. The micrograph of LG40 sample exhibits agglomerate sizes bigger than $6\ \mu\text{m}$, with grained aspect. The particle size is between 300 and 600 nm.

The distribution of different elements was analysed by means of EDX analysis. The results indicate an homogeneous distribution of chromium and calcium in samples which is in agreement with the formation of the Ca,Cr:LGG solid solution, as previously discussed. A representative mapping analysis of LG40 sample is given in Fig. 7, also indicating a homogenous distribution of elements, though some regions of heterogeneity in calcium and gallium are observed. These results are in

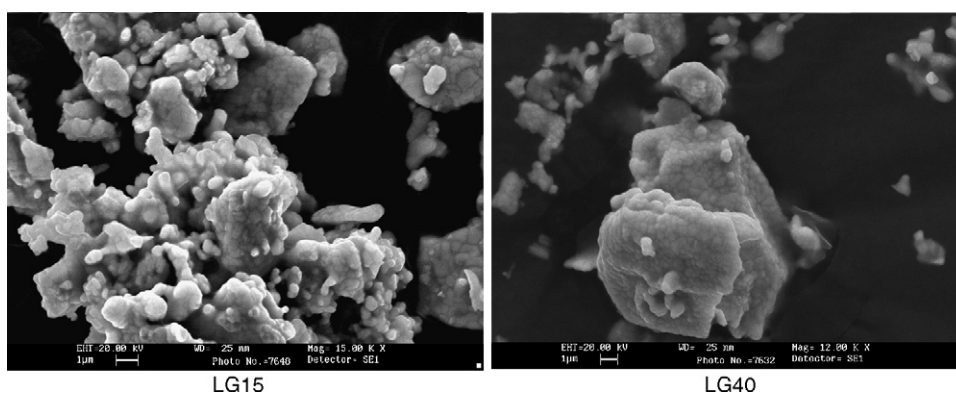


Fig. 6. SEM micrographs of representative powders fired at $1250^\circ\text{C}/6\text{ h}$.

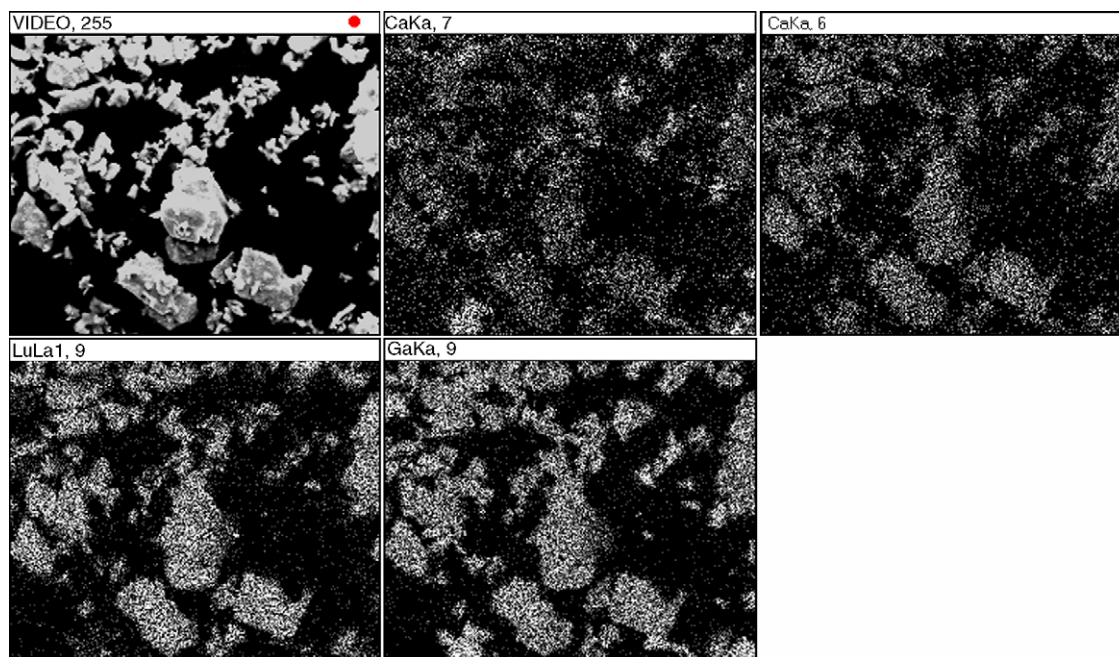


Fig. 7. EDX mapping of LG40 sample fired at 1250 °C/6 h.

accordance with the presence of Ga_2O_3 detected by XRD and with the entrance of Cr(III) substituting for Ga(III) at higher chromium concentrations.

4. Conclusions

From the above discussion, the following conclusions may be drawn:

1. A solid solution of Ca^{2+} and Cr^{4+} substituting for Lu^{3+} in dodecahedral sites $\text{Ca}_x\text{Cr}_x\text{Lu}_{3-2x}\text{Ga}_5\text{O}_{12}$ up to $x=0.2$ has been synthesised by solid state reaction of raw oxides. The solid solution exhibits a pink colour.
2. When $\text{Ca}_x\text{Cr}_x\text{Lu}_{3-2x}\text{Ga}_5\text{O}_{12}$ is saturated above $x=0.2$ composition, Cr^{3+} is in octahedral positions substituting for Ga^{3+} and the colour of samples become green.
3. In the absence of calcium as charge compensator, the Cr(IV) is not stabilised and the Cr(III) enters in octahedral sites substituting for Ga(III), generating a green colour in samples.
4. New solid solution is stable in ceramic glaze matrix, indicating that can be used as a new pink ceramic pigment.

Acknowledgements

Authors gratefully acknowledge the financial support of Spanish CICYT (MAT 2005 program) and Fundación Caja de Castellón Bancaixa.

References

1. Hua, H., Mirov, S. and Vohra, Y. K., High-pressure and high-temperature studies on oxide garnets. *Phys. Rev. B*, 1996, **54**(9), 6200–6209.
2. Xu, Y. N., Ching, W. Y. and Briceen, B. K., Electronic structure and bonding in garnet crystals $\text{Gd}_3\text{Sc}_2\text{Ga}_3\text{O}_{12}$ (GSGG), $\text{Gd}_3\text{Sc}_2\text{Al}_3\text{O}_{12}$ (GSAG) and

- $\text{Gd}_3\text{Ga}_5\text{O}_{12}$ (GGG) and with comparison to $\text{Y}_3\text{Al}_5\text{O}_{12}$ (YAG). *Phys. Rev. B*, 2000, **61**, 1817–1824.
3. Ehrentraut, D., Growth of lattice-matched yttrium-substituted aluminium garnets for zone-doped crystals. *J. Cryst. Growth*, 2002, **242**, 375–382.
4. Kück, S., Petermann, K., Pohlmann, U. and Huber, G., *Phys. Rev. B*, 1995, **51**(24), 17323–17331.
5. Brandle, C. D. and Barns, R. L., An Empirical formula for the calculation of lattice constants of oxide garnets based on substituted yttrium-gadolinium-iron garnets. *J. Cryst. Growth*, 1974, **26**, 169.
6. Özen, G., Belin, B., Yildirim, G. and Güven, H., Lanthanum lutetium gallium garnets doped with Cr^{+3} and Nd^{+3} ions: analyses of elemental composition and energy transfer. *Opt. Commun.*, 2000, **173**, 341–347.
7. Padlyak, B. V., Grinberg, M., Lukaszewicz, T., Kisielewski, J. and Swirkowicz, M., EPR spectroscopy of the Cr^{+3} centers in LLGG:Cr single crystals. *J. Alloys Comp.*, 2003, **361**, 6–12.
8. Ogino, H., Yoshikawa, A., Lee, J.-H., Niké, M., Solovieva, N. and Fukuda, T., Growth and characterization Yb^{+3} doped garnet crystals for scintillator application. *Opt. Mater.*, 2004, **26**, 535–539.
9. Shirinyan, G., Ovanesyan, K. L., Eganyan, A., Petrosyan, A. G., Pedrini, C., Dujardin, C. et al., X-ray and optical studies of ytterbium-doped gallium garnets. *Nucl. Instrum. Meth. A*, 2005, **537**, 134–138.
10. Matkovskii, A., Potera, P., Sugak, D., Grigorjeva, L., Millers, D., Pankratov, V. et al., Stable and transient colour centers in $\text{Gd}_3\text{Ga}_5\text{O}_{12}$ crystals. *Cryst. Res. Technol.*, 2004, **39**(9), 788–795.
11. Chen, J.-Ch., Lo, Ch.-Y., Huang, K.-Y., Kao, F.-J., Tu, Sh.-Y. and Huang, Sh.-L., Fluorescence mapping of oxidation states of Cr ions in YAG crystal fibers. *J. Cryst. Growth*, 2005, **274**, 522–529.
12. Feldman, R., Shimony, Y. and Burshtein, Z., Dynamics of chromium ion valence transformations in Cr,Ca:YAG crystals used as laser gain and passive Q-switching media. *Opt. Mater.*, 2003, **24**, 333–344.
13. Eilers, H., Hömmerich, U., Jacobsen, S. M., Yen, W. M., Hoffman, K. R. and Jia, W., Spectroscopy and dynamic of $\text{Cr}^{+4}:\text{Y}_3\text{Al}_5\text{O}_{12}$. *Phys. Rev. B*, 1994, **49**(22), 15505–15513.
14. Baldi G. and Dolen N., Synthesis of a new class of red pigments based on perovskite type for use in body stain and high temperature glazes, *Int. Ceram. J. Suppl. Ceramica Informazione*, Faenza, 2000. April, 31.
15. Monrós, G., Badenes, J. A., García A. and Tena M. A. “El colour de la cerámica: nuevos mecanismos para los nuevos procesos de la industria cerámica”, Atenea 11, Castellón, 2003. p. 150.

16. Monrós, G., Pinto, H., Badenes, J. A., Llusar, M. and Tena, M. A., Chromium (IV) stabilisation in new ceramic matrice by coprecipitation method: application as ceramic pigments. *Z. Anorg. Allg. Chem.*, 2005, **631**, 2131–2135.
17. POWCAL-LSQC Programmes, Ptt. Of Chemistry, Abberdeen University (U.K.).
18. CIE, *Recommendations on Uniform Colour Spaces, Colour Difference Equations*. Psychometrics Colour Terms. Supplement no. 2 of CIE Publ. No. 715 (E1–131) 1971. Bureau Central de la CIE, Paris, 1978.
19. Sugano, S., Tanabe, Y. and Kamimura, H., *Multiplets of Transition Metal ions in crystals*. Academic Press, New York, 1970.
20. Shannon, R. D., *Acta Crystallogr.*, 1976, **A32**(5), 751–767.